Technical report, IDE1206, March 2012

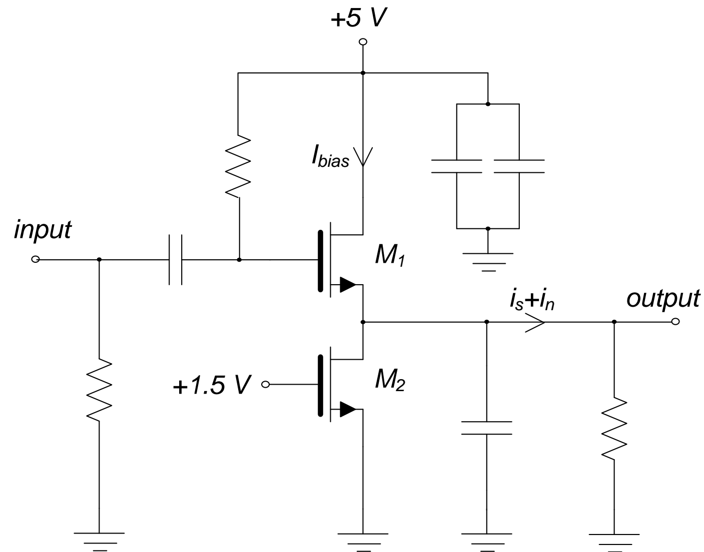

Noise measurements of a low power detector for RFID applications

Master`s thesis in Microelectronics and Photonics

Denis Belenko

Supervised by: Emil Nilsson

School of Information Science, Computer and Electrical Engineering

Abstract

In this work we provide measurements on low power envelope detector and compare them with results predicted by theory. This envelope detector is supposed to be used as a part of low power Wake-up radio for RFID applications. In the work we were mostly interested in noise parameters and blocker effect verification.

The detector we use is based on CMOS transistors biased in subthreshold region. It gives us low power consumption and high sensitivity. For power consumption about 10 uA and signal to noise ratio equals to 10, the achieved sensitivity is 1.8 mV.

The results of the work can be used to build low power envelope detector for specific requirements.

Table of contents

Abstract 2
1 Introduction 4
2 Theory 6
2.1 Basic theory of the MOSFET 6
2.1.1 Introduction 6
2.1.2 The MOSFET 7
2.1.3 I/V characteristic of the MOSFET 8
2.1.4 Second order effects 12
2.2 Detector theory 15
2.2.1 Introduction 15
2.2.2 Signal detection 16
2.2.3 Blocker effect 16
3 Setup and experiments 18
3.1 Setup overview 18
3.2 Signal interfacing circuit 18
3.3 Amplifier 20
3.4 Detector 23
4 Results 27
4.1 DC measurements 27
4.2 Signal detection 28
4.3 Blocker effect 29
5 Conclusion 31
References 32

1 Introduction

In modern times the increasing complexity of wireless systems requires more effective techniques of signal detecting.

For some applications, for example, RFID and wireless sensor systems, ultra low power consumption is usually preferable than high performance and capacity of the radio channel. To satisfy this challenge we have to use the simplest forms of radio receiver, which works at low data rate with simple modulation signals, for example, OOK (on-off keying) modulation [1], which is robust non-coherent modulation.

Such radio can be used to receive data at low rate or as wake-up radio, which is waiting for wake up signal. After detecting this signal it can run more sophisticated and power demanding blocks of the receiver. The only requirements for such radio system are ultra low power consumption, reliable functionality and a reasonable sensitivity.

OOK is the simplest form of amplitude-shift keying (ASK) modulation that represents digital data as the presence or absence of a carrier wave. Power consumption in such case is very low because this modulation does not require an always running local oscillator at the receivers part.

OOK is more spectrally efficient than frequency-shift keying (FSK), but more sensitive to noise.

In this work we only consider detector part for such type of radio. For detecting OOK signal we can use ordinary envelope detector, which basically consist of two blocks – nonlinear part to produce number of harmonics from RF signal, linear part to filter out higher harmonics and to keep only demodulated signal.

In our case we do not want to use diode detector, which is the simplest form of envelope detector, because normally operational point of the diode has to be chosen at quite big bias current. The solution is to use effect of subthreshold con-

duction in the MOSFET. This effect gives us opportunity to build extremely low power envelope detector with essential sensitivity [2].

The main aims of this work were to built a low power detector and provide measurements on it using instruments for RF measurements: signal and noise generators, vector network analyzer, spectrum analyzer and oscilloscope. Results of the measurement were also verified with theoretical expressions for such type of detector. In addition a low noise measurement amplifier and signal interfacing electronics were built.

In the next chapter we will have a brief overview of the MOSFET basics. Some sources give theoretical explanation of the physical processes inside the transistor [3], while other gives examples of computer modeling of the MOS transistor [4]. After it we will consider theory of the envelope detector based on MOS transistors [5], schematics of additional blocks and complete setup for providing experiments.

2 Theory

2.1 Basic theory of the MOSFET

2.1.1 Introduction

A MOS (**M**etal **O**xide **S**emiconductor) structure is obtained by growing a thin layer of insulator (SiO_2) on top of silicon substrate, and depositing a metal layer on the insulator, as it is shown in Figure 2.1.1, where *d* is the thickness of the insulator layer and *V* is the applied voltage.

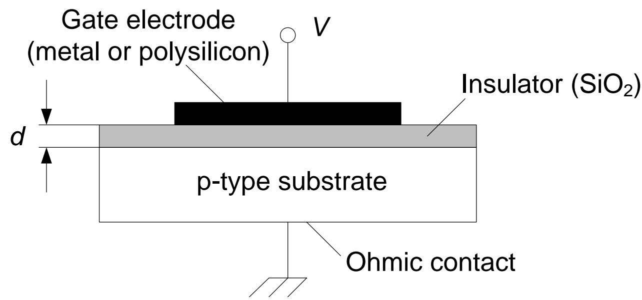

Figure 2.1.1 Cross section of a MOS diode

Let us consider the energy band diagram of an ideal p-type MOS diode with zero voltage applied as shown in Figure 2.1.2. At zero bias, there is no energy difference between the metal work function $q\phi_m$ and the semiconductor work function $q\phi_s$, therefore, the work function difference $q\phi_{ms}$ is zero [3]

$$q\phi_{ms} = (q\phi_m - q\phi_s) = q\phi_m - (q\chi + \frac{E_g}{2} + q\psi_B) = 0, \qquad (2.1.1)$$

where $(q\chi + \frac{E_g}{2} + q\psi_B)$ is equal to $q\phi_s$,

$q\chi$ – is the electron affinity,

E_g – is the semiconductor bandgap,

$q\psi_B$ – is the energy difference between the Fermi level E_F and the intrinsic Fermi level E_i.

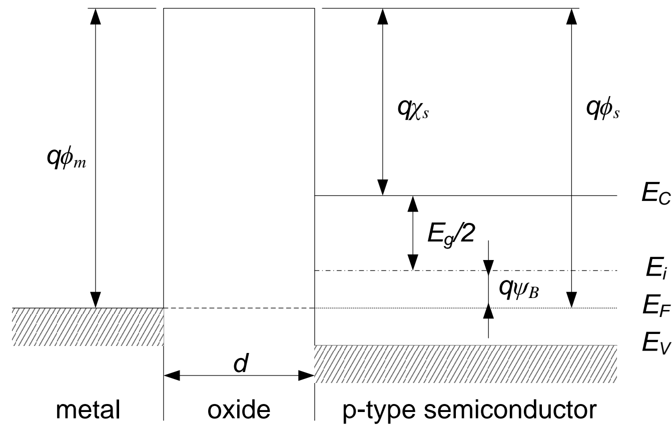

Figure 2.1.2 Energy band diagram of an ideal MOS diode at *V=0*

The voltage applied across a MOS structure controls the state of the Si-surface underneath. Depending on the voltage sign there can be two states of the MOS diode – *accumulation* and *inversion*. It can be used to make a voltage-controlled switch. *Accumulation* state occurs when a negative voltage is applied over the gate, that attracts the holes from the p-type silicon to the surface; and the *inversion* state – a positive voltage (larger than the threshold voltage) applied creates an inverted layer of electrons at the surface. The *threshold voltage* is the gate voltage at which the volume density of electrons in the inversion layer is the same as the volume density of holes in the body.

2.1.2 The MOSFET

The basic part of a MOSFET (Metal Oxide Semiconductor Field Effect Transistor) (Figure 2.1.3) is the MOS diode. MOSFET is a three terminal device. The gate electrode is formed on top of the MOS diode. Inside the substrate there are also two heavily doped regions: *source* and *drain*, with metal electrodes above. The source-to-drain electrodes are equivalent to two p-n junctions that are connected back-to-back. The central MOS diode is used to create and control the inverted channel, which connects the source and drain junctions. The current flow between the source and the drain is thus controlled by an electric field created by a voltage V_g applied between the gate electrode and the bulk of the transistor. The

MOSFET may be n-channel or p-channel depending on the type of majority carriers in the channel region.

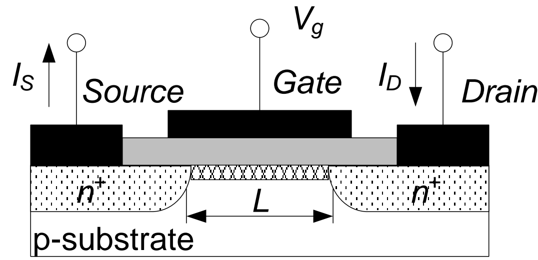

Figure 2.1.3 Cross section of n-channel MOSFET

The dimension of the gate along the source-drain path is called the length, *L* (effective length), and that perpendicular to the length is called the width, *W*.

If with zero voltage applied to the gate there is no conduction channel between the drain and source regions, the MOSFET is referred to as a *normally-off device (an enhancement-mode device)*. A certain minimum gate voltage (threshold voltage V_{th}) should be applied to induce a conduction channel.

There is also another type of MOSFET called *depletion-mode device* (*normally-on device*). These are MOSFET devices that are doped so that a channel exists even with zero gate voltage. In order to control the channel, a negative voltage is applied to the gate (for an n-channel device), depleting the channel, which reduces the current flow through the device.

2.1.3 I/V characteristic of the MOSFET

In reality, the turn-on phenomenon is a gradual function of the gate voltage, making it difficult to define V_{th} explicitly. In semiconductor physics, the V_{th} of an n-channel MOSFET is usually defined as the gate voltage for which the interface is "as much n-type as the substrate is p-type" [3]

$$V_{th} = V_{FB} + 2\psi_B + \frac{\sqrt{2\varepsilon_s q N_A (2\psi_B + V_{BS})}}{C_0} \approx 2\psi_B + \frac{\sqrt{2\varepsilon_s q N_A (2\psi_B)}}{C_0}, \qquad (2.1.2)$$

where V_{FB} – is the flat-band voltage,

ε_s – is the dielectric constant of silicon,

N_A – is the doping concentration of the substrate,

V_{BS} – is the reverse substrate-source bias,

C_0 – is the gate oxide capacitance per unit area.

Assume in approximate analysis that the device turns on abruptly for $V_{gs} \geq V_{th}$.

Triode region

Suppose the drain voltage to be greater than zero (Figure 2.1.4 a). Relations between drain current and applied voltages can be expressed as [6]

$$I_D = \mu_n C_0 \frac{W}{L}\left[(V_{gs} - V_{th})V_{ds} - \frac{1}{2}V_{ds}^2\right], \qquad (2.1.3)$$

where μ_n – is the mobility of charge carriers.

The peak of the current given by (2.1.3) occurs at $V_{ds} = V_{gs} - V_{th}$ and the peak current is

$$I_{D\max} = \frac{1}{2}\mu_n C_0 \frac{W}{L}(V_{gs} - V_{th})^2, \qquad (2.1.4)$$

where $(V_{gs} - V_{th})$ – is called "overdrive voltage",

$\frac{W}{L}$ – is called the "aspect ratio".

If $V_{ds} \leq V_{gs} - V_{th}$, we say the device operates in the "triode region".

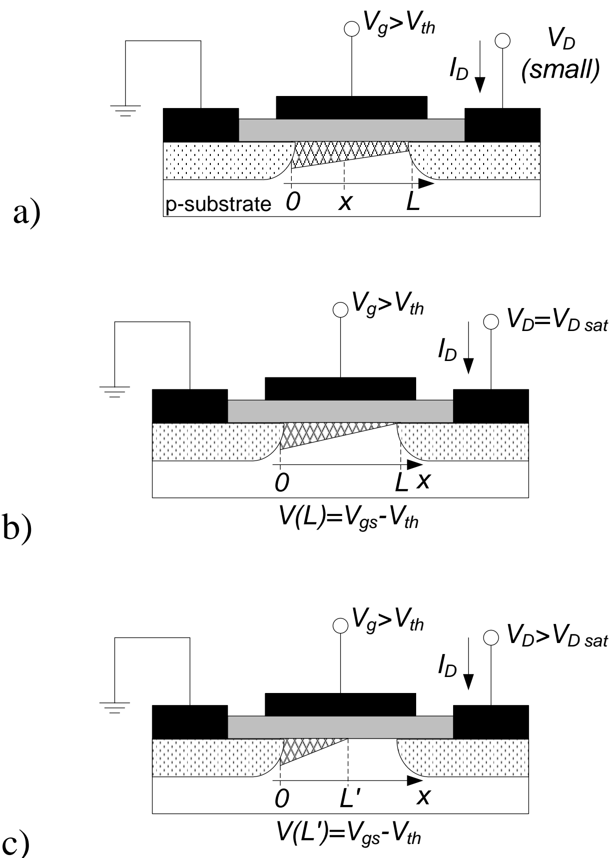

Figure 2.1.4 Operations of the MOSFET

a) Low drain voltage

b) Pinch-off point

c) Saturation region

If in (2.1.3), $V_{ds} \ll 2(V_{gs} - V_{th})$, we have

$$I_D \approx \mu_n C_0 \frac{W}{L}(V_{gs} - V_{th})V_{ds}, \tag{2.1.5}$$

that is, the drain current is a linear function of V_{ds}. The linear relationship implies that the path from the source to the drain can be represented by a linear resistor equal to

$$R_{on} = \frac{1}{\mu_n C_0 \frac{W}{L}(V_{gs} - V_{th})}. \tag{2.1.6}$$

With the condition $V_{ds} \ll 2(V_{gs} - V_{th})$, we say the device operates in deep triode region (Figure 2.1.5).

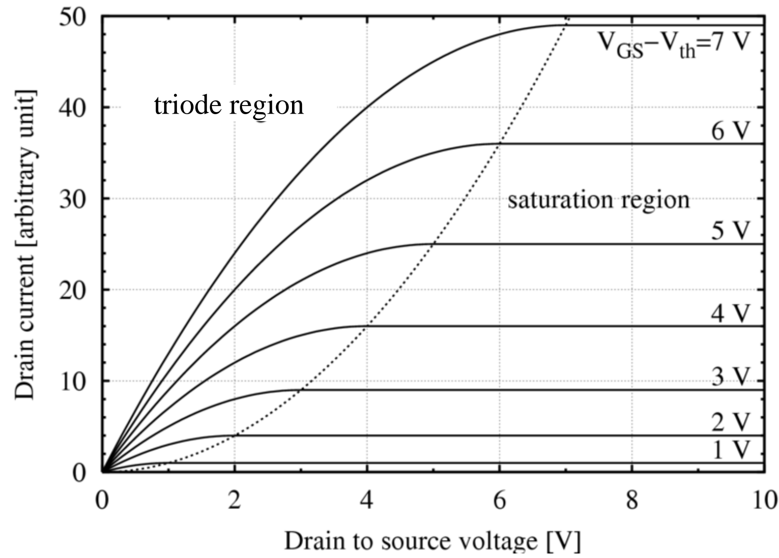

Figure 2.1.5 Idealized drain characteristic of a MOSFET

Saturation region

When $V_{gs} > V_{th}$ and $V_D > (V_{gs} - V_{th})$, the switch is turned on, and a channel has been created, which allows current to flow between the drain and source. Since the drain voltage is higher than the gate voltage, the electrons spread out, and conduction is not through a narrow channel but through a broader, two- or three-dimensional current distribution extending away from the interface and deeper in the substrate. The onset of this region is also known as pinch-off (see Figure 2.1.4 b) to indicate the lack of channel region near the drain. The drain current is now weakly dependent upon drain voltage and controlled primarily by the gate-source voltage. If the voltage $V_{D\ sat}$ increases beyond pinch-off, the pinch-off region between the channel pinch-off point and drain region causes the effective channel length to decrease from L to L' (see Figure 2.1.4 c).

$$I_D = \frac{1}{2}\mu_n C_0 \frac{W}{L'}(V_{gs} - V_{th})^2. \qquad (2.1.7)$$

With the approximation $L \approx L'$, a saturated MOSFET can be used as a current source connected between the drain and the source.

2.1.4 Second-order effects

Body effect

In previous expressions it was assumed that the bulk and the source of the MOSFET were connected to ground. But if the bulk voltage, V_B, drops below the source voltage (see Figure 2.1.6) the body effect occurs. The threshold voltage changes with respect to potential difference between source and bulk.

$$V_{th} = V_{th0} + \gamma(\sqrt{|2\psi_B - V_B|} - \sqrt{|2\psi_B|}), \tag{2.1.8}$$

where V_{th0} – is given by (2.1.2),

$\gamma = \frac{\sqrt{2\varepsilon_s q N_A}}{C_0}$ – is the body effect coefficient.

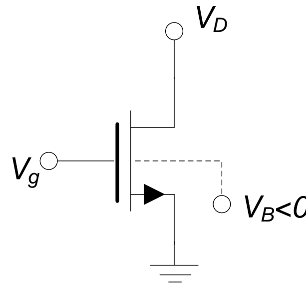

Figure 2.1.1 NMOS device with negative bulk voltage

Channel-length modulation

The actual length of the inverted channel gradually decreases as the potential difference between the gate and the drain increases. In other words, in (2.1.7), L' is in fact a function of V_{ds}. This effect is called "channel-length modulation". Assuming first-order relationship between $\Delta L / L$, where $\Delta L = L - L'$, and V_{ds} such as $\Delta L / L = \lambda V_{ds}$, we have, in saturation,

$$I_D = \frac{1}{2}\mu_n C_0 \frac{W}{L}(V_{gs} - V_{th})^2(1 + \lambda V_{ds}). \tag{2.1.9}$$

where λ – is the channel-length modulation coefficient.

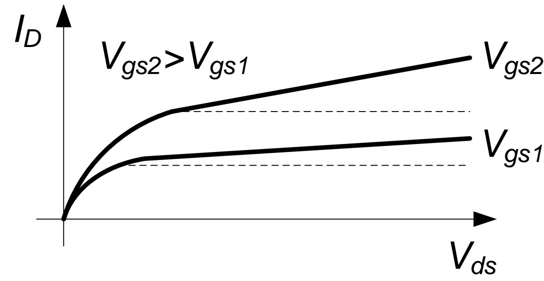

Figure 2.1.2 Finite saturation region slope resulting from channel-length modulation

Subthreshold conduction

Earlier we have assumed that the device turns off abruptly as V_{gs} drops below V_{th}, but in reality, for $V_{gs} = V_{th}$, a "weak" inversion layer still exists and some current flows from drain to source. Even for $V_{gs} < V_{th}$, I_D is finite, but it exhibits an exponential dependence on V_{gs} [3]

$$I_D = I_{D0} e^{V_{gs}/V_0}, \qquad (2.1.10)$$

where $V_0 = \frac{nkT}{q}$ with 1<n<2,

n – is an nonideality factor.

The subthreshold conduction is particularly important when the MOSFET is used as a low-voltage, low-power device, such as a switch in digital logic and memory applications, because the subthreshold conduction describes how the switch turns on and off.

Subthreshold conduction is extremely important for the rest of this work, because it gives as necessary nonlinearity for the detection and also keeping transistor in subthreshold region provide low-power consumption [5].

Breakdown

When V_{ds} increases, the transistor can enter a region where I_{ds} suddenly increases until breakdown of the drain-to-substrate p-n junction occurs. The break-

down is caused by the high electric field in the drain end. In short channel devices, this is called *hot-carrier effect,* due to the high electric field at the drain end, and it can also result in device breakdown [6].

2.2 Detector theory

2.2.1 Introduction

From the equation (2.1.10) we can see that drain current of the MOSFET transistor in subthreshold region exponentially depends on gate voltage. So we can use this part of I/V characteristic to detect signal, it will also provide low power consumption, because normally subthreshold currents are low. Schematic of such detector is shown at Figure 2.2.1.

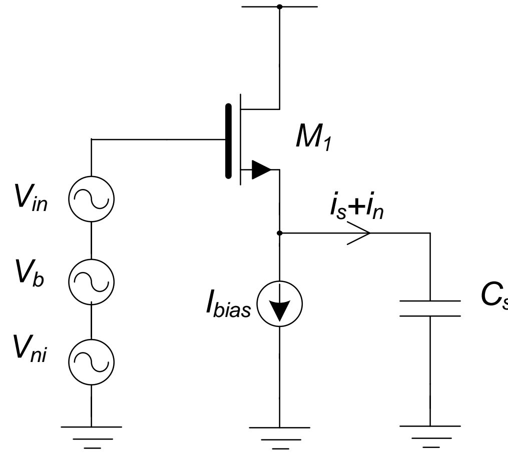

Figure 2.2.1 Ideal envelope detector schematic

Current source, I_{bias}, is used to create stable bias conditions for the transistor *M1*. Capacitor, C_s, is charged by output current, which also create output voltage.

Assuming any DC current being included in I_{D0}, we may expand (2.1.10) as

$$I_D = I_{D0} + \frac{dI_D}{dV_g} V_g + \frac{d^2 I_D}{dV_g^2} \frac{V_g^2}{2}, \tag{2.2.1}$$

where V_g – is signal applied between gate and source of the transistor,

$$\frac{d^2 I_D}{dV_g^2} = \frac{I_{D0}}{V_0^2},$$

$$\frac{dI_D}{dV_g} = \frac{I_{D0}}{V_0} = g_m$$ – transconductance.

From expressions (2.1.10) and (2.2.1) we can obtain relations between input signal and output current [5]. But Taylor`s series (2.2.1) is correct only for small levels of input signals. If we want to get correct model for larger amplitudes of input signal we can use exponent expansion in a Fourier series:

$$e^{A\cos(\omega t)} = I_0(A) + 2I_1(A)\cos(\omega t) + 2I_2(A)\cos(2\omega t) + ... \tag{2.2.2}$$

Where I_n is modified Bessel function of the first kind.

2.2.2 Signal detection

Assume that AM modulated signal is applied to the input of ideal detector:

$$V_{in} = V_m \frac{1+\sin\omega_m t}{2}\cos\omega t. \tag{2.2.3}$$

Then using (2.1.10) and (2.2.1) or (2.2.2) we can get an expression for the detected signal amplitude at angular frequency ω_m

$$i_{sm} = \frac{1}{8}\frac{I_{do}}{V_0^2}V_m^2 \tag{2.2.4}$$

or

$$i_{sm} = 4I_{bias}\frac{I_1(V_m/2V_0)I_1(V_m/4V_0)}{I_0(V_m/2V_0)I_0(V_m/4V_0)}. \tag{2.2.5}$$

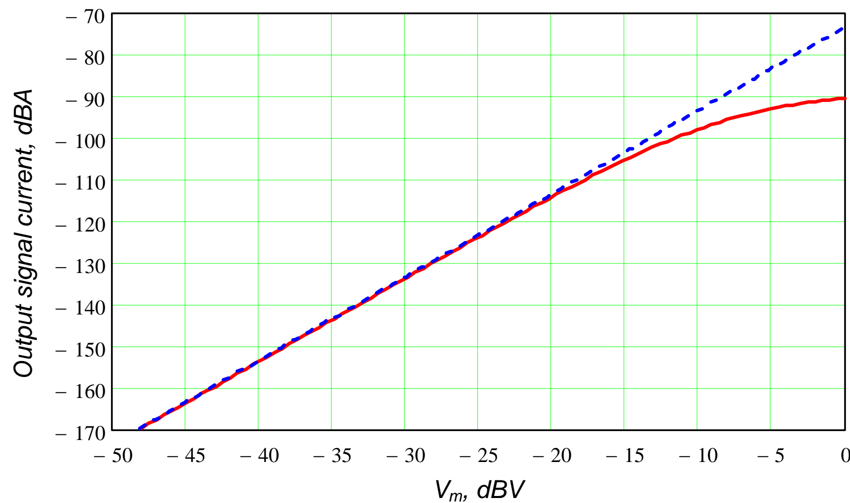

Figure 2.2.2 Signal detection

At the Figure 2.2.2 we can see that these expressions give different results only for large amplitudes of input signal.

2.2.3 Blocker effect

At the input of our detector there is a superposition of modulated signal, V_{in}, blocker signal, V_b, and noise distributed around the blocker, V_{ni}. Due to nonlinearity in the transistor, part of this noise is mixed with blocker signal and can be downconverted to the baseband of the detector (see Figure 2.2.3). This is called blocker effect and can be described by following expression [5]

$$\mathrm{i}_{\mathrm{nb}}^{2} = 2\mathrm{I}_{\mathrm{bias}}^{2} \frac{I_{1}^{2}(\mathrm{V_b}/\mathrm{V_0})}{I_{0}^{2}(\mathrm{V_b}/\mathrm{V_0})} \frac{\mathrm{V}_{\mathrm{ni}}^{2}}{\mathrm{V}_{0}^{2}}. \tag{2.6}$$

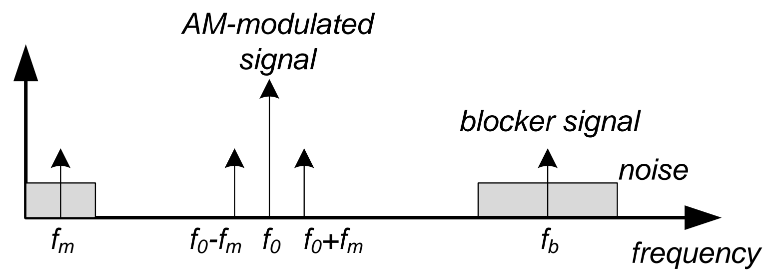

Figure 2.2.3 Blocker effect

3 Setup and experiments

3.1 Setup overview

The aim of this thesis is to build an envelope detector, to test it and then to compare results with the theory described in previous chapter.

Some measurements are supposed to be provided at relatively low levels of the input signal, with the minimum value -60 dBV. Therefore, the minimum value of output current is expected to be in the order of -190 dBA. To be able to register such weak signals with ordinary oscilloscope in the lab we have to amplify it with low noise amplifier before.

Another important point is that we want to provide measurements with a superposition of different signals at detectors input: modulated signal, blocker signal and noise. This is addressed by a signal interfacing circuit (Figure 3.1), placed in front of the detector. This circuit enables us to sum different signals and to control it using spectrum analyzer. To decrease influence of different input sources on each other we put in -10 dB attenuators. This provides additional RF isolation between inputs. Signal from the source passes attenuator and reaches signal interfacing circuit, at this point the signal is -10 dB attenuated. In the signal interfacing circuit signals from different sources are combined and then applied to detector, but by some reasons part of the signal can be reflected back to the source and also signal from the first source can reach second and vice versa. This reflected signal passes attenuator once again so it becomes -20 dB attenuated.

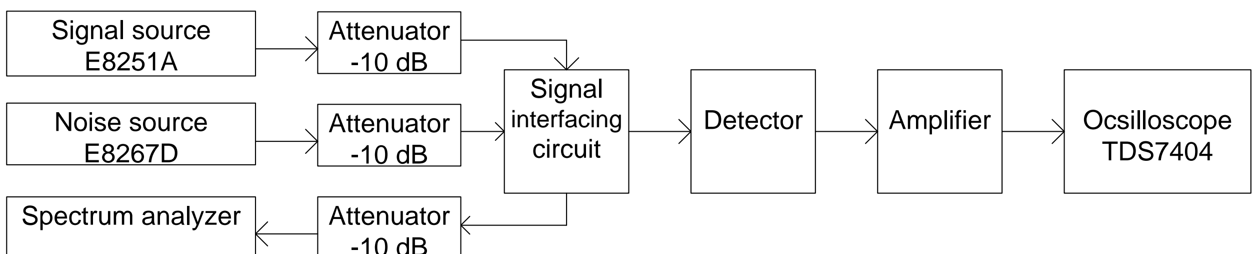

Figure 3.1 Measurements setup

3.2 Signal interfacing circuit

All devices that we use for measurements have input-output ports with 50 Ω real impedance, so it is preferable to use signal interfacing circuit with such input impedance.

As a basis for signal interfacing circuit we use slightly changed three-port resistive "Wye" splitter (see Figure 3.2). Ports 1, 2 and 3 are preserved from the "Wye" splitter and have impedance matched to 50 Ω. Port 4 is connected to common point of the "Wye" splitter and it has 22.7 Ω real impedance value. Ports 1, 2 and 3 are used to connect signal source, noise source and spectrum analyzer, port 4 is used as output.

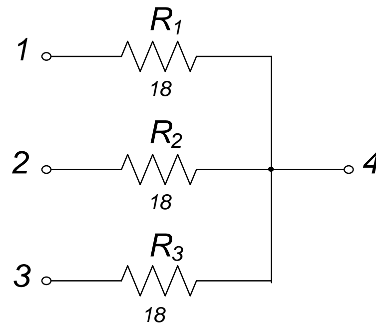

Figure 3.2 Signal mixer based on resistive Wye splitter

Transfer function from each of three ports (1, 2 and 3) to the port 4 is $V_{out} \approx 0.654 V_{in}$. While isolation between each of 1, 2 or 3 port and any other of them is about -6.02 dB – where -3.0103 dB is real resistive loss and -3.0103 dB is power splitting between two other ports.

This type of resistive power mixer can be made very compact, and is naturally wideband, working down to zero frequency (DC). Measured S-parameters for such device are shown at Figure 3.3. The lowest frequency at the figure is not zero, because 10 MHz is the lowest frequency of the network analyzer we used.

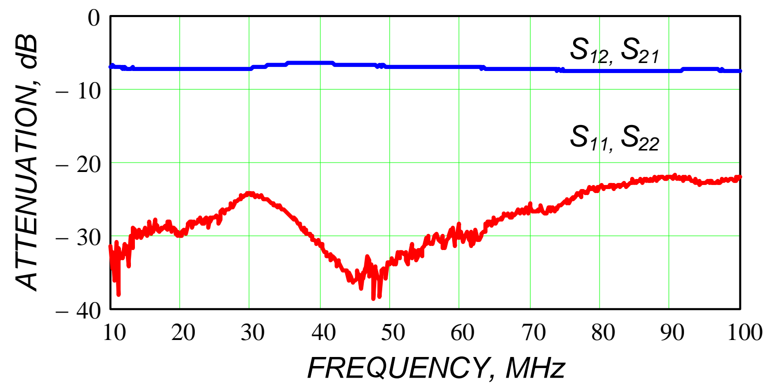

Figure 3.3 Signal mixer S-parameters

3.3 Amplifier

Detector output signal consist of big amount of different harmonics due to nonlinear process in it. We are interested only in information part of the signal, therefore, we have to filter out high frequencies and DC component from it. Since detected signal is weak we should also amplify it to be able to measure parameters of the signal and noise.

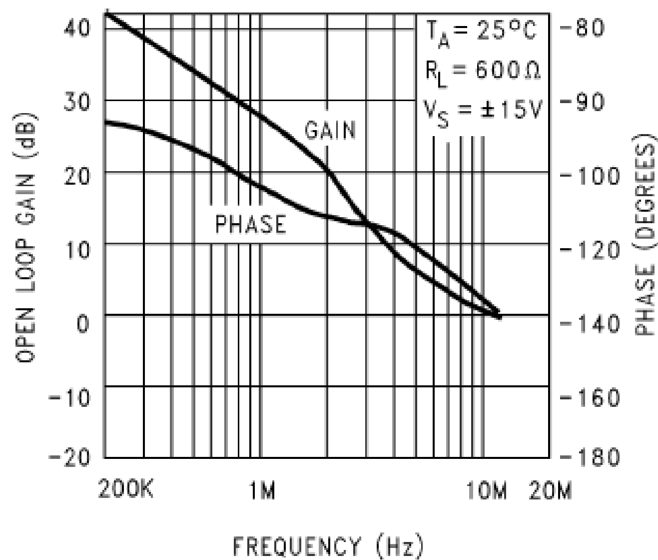

Figure 3.4 Open Loop Gain & Phase vs Frequency

For test purposes the simple way to built amplifier is to use an operational amplifier. It will also provide filtering functions due to internal construction of operational amplifier. For our measurements we choose LM837. It has low input noise voltage – 4.5 nV/√Hz, so for bandwidth 1 MHz it will produce equivalent

noise at the input ≈ 4.5 uV. From the Figure 3.4 we can choose necessary amplification for our bandwidth.

For our measurements we decide to built double stage amplifier (see Figure 3.5), this provides necessary bandwidth and amplification. First stage is AC amplifier [7], while second is simple noninverting amplifier. This amplifier has big input impedance

$$Z_{in}(\omega) = \sqrt{(R_1 + R_2)^2 + (\omega C_2 R_1 R_2 - \frac{1}{\omega C_1})^2} \tag{3.1}$$

where ω – is radian frequency.

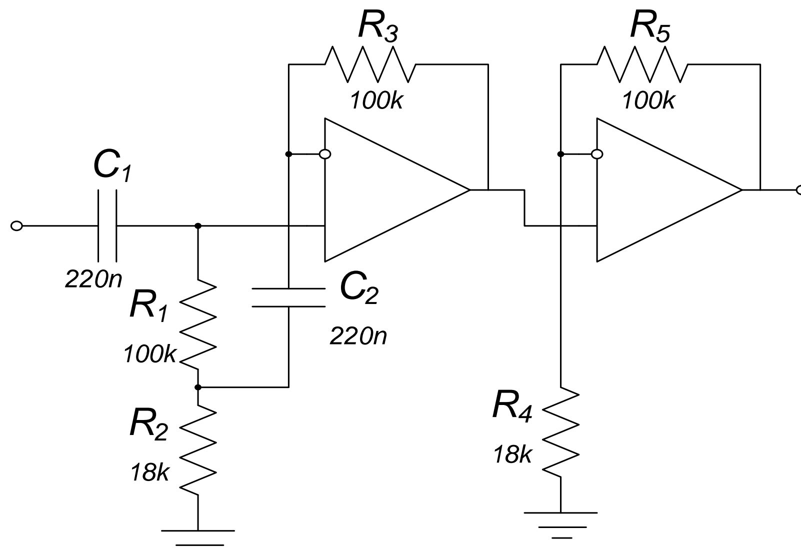

Figure 3.5 Double stage amplifier

As we see from (3.1) input impedance of the amplifier depends on signal frequency.

Capacitor C_1 is used only not to allow DC component of input current to reach operational amplifier and almost does not change lowest frequency of the bandwidth.

Capacitor C_2 provides 100% negative DC feedback, it allows to keep almost zero value of DC component in the output voltage.

Total amplification can be expressed as

$$A(p)=\frac{1+\frac{R_3}{R_2}+\frac{1}{pC_2R_1}+\frac{1}{pC_2R_2}}{1+\frac{1}{pC_2R_1}+\frac{1}{pC_2R_2}+\frac{1}{p^2C_1C_2R_1R_2}}\cdot\left(1+\frac{R_5}{R_4}\right) \tag{3.2}$$

where p – is Laplace operator.

The Laplace transform is often used in circuit analysis, it allows to describe relations between input and output signals in the circuit in frequency-domain, where inputs and outputs are functions of complex angular frequency. Applying inverse Laplace transform it is possible to obtain circuit characteristic in time domain. The Laplace transform has the useful property that many relationships and operations over the originals in time domain correspond to simpler relationships and operations over the images in frequency domain [8].

At the Figure 3.6 we can see measured frequency response of the amplifier. There is a peak near 1 MHz frequency, one can use properly tuned filter to compensate it and to avoid probably unwanted oscillations at this frequency. But during our measurements we noticed that there were no self oscillations and results remains proper, so we did not use any technique change frequency response characteristic around 1 MHz.

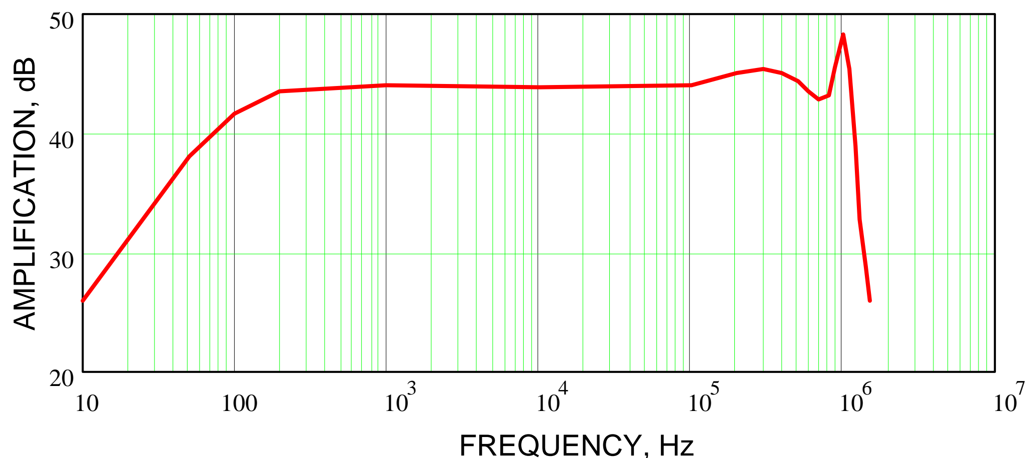

Figure 3.6 Amplifier frequency response

Measured input impedance of the amplifier for 1 kHz harmonic signal is about 2.45 MΩ (see Figure 3.7), this value coincides with expression (3.1).

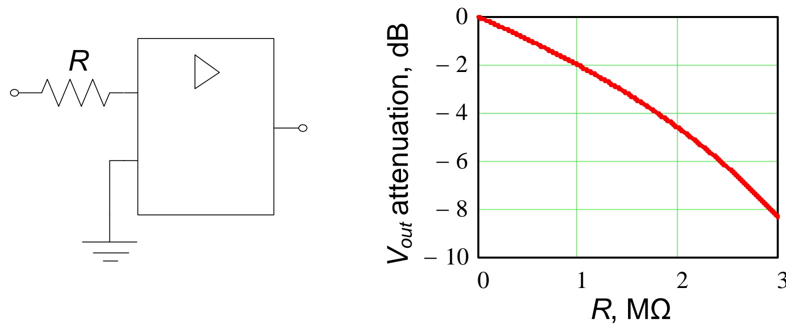

Figure 3.7 Input impedance measurement – Setup & Results

3.4 Detector

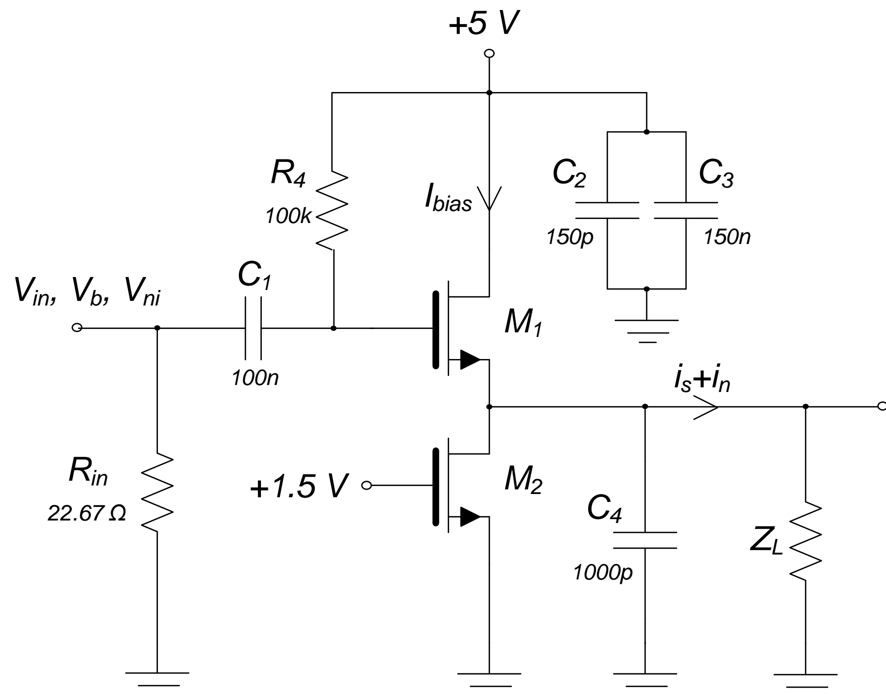

Figure 3.8 Detector schematic

Detector used for measurements is presented at the Figure 3.8, where R_{in} – is output impedance of the signal mixer, Z_L – is input impedance of the amplifier. This setup is a bit different from ideal, described in previous chapter. Capacitor C_1 filters out DC component from the input signal. C_2 and C_3 are decoupling capacitors, they are used to stabilize supply voltage. Capacitor C_4 implements filtering

function, it filers out high frequencies from the output signal and saves only information part of it. Transistor M_2 is biased in saturation and acts as a controlled current source, while M_1 performs detecting functions. Resistor R_4 is needed to set correct operation point, we can control operation voltage automatically by changing bias current.

Source follower

From the Figure 3.8 we can see that transistors M_1 and M_2 are connected under the scheme of source follower. Using the source follower equivalent circuit (see Figure 3.9) [6] we can obtain all main parameters of our detector.

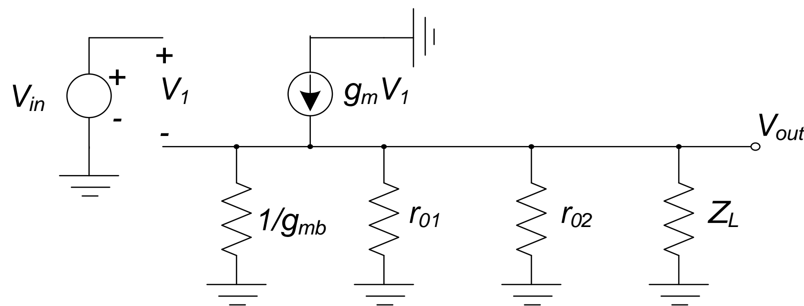

Figure 3.9 Source follower small-signal equivalent circuit

In the Figure 3.9 conductance g_{mb} represent body effect (1.8), but in transistors that we use bulk is connected to source, so $g_{mb}=0$. Ideal current source, g_mV_1, represents I/V characteristic of the first transistor, where trasconductance, g_m, is defined by equation – $g_m = \partial I_D / \partial V_g = I_D / V_0$. Equivalent resistor Z_L represent load of the detector and resistors r_{01}, r_{02} represents channel-length modulation effect (1.9).

$$r_0 = \frac{1}{\partial I_D / \partial V_{ds}} = \frac{1}{\frac{1}{2}\mu_n C_0 \frac{W}{L}(V_{gs} - V_{th})^2 \lambda} \approx \frac{1}{\lambda I_D}. \tag{3.3}$$

From the equivalent circuit in Figure 3.9 we can see that there is 100% negative voltage feedback. That will change output impedance of the circuit (see Figure 3.10), where

$$R_{out} = \frac{1}{g_m}. \tag{3.4}$$

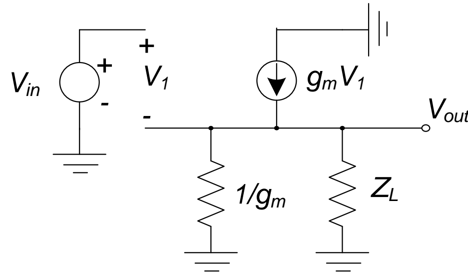

Figure 3.10 Modified source follower small-signal equivalent circuit

From the Figure 3.10 we can find that

$$A_V = \frac{\frac{1}{g_m} \| Z_L}{\frac{1}{g_m} \| Z_L + \frac{1}{g_m}}. \quad (3.5)$$

Blocker effect

For the circuit of ideal detector (2.2.1) blocker effect can be described by expression (2.2.6).

In reality we can not measure current directly, therefore, we have to measure output voltage of the noise and then estimate by calculations noise current. From the Figure (3.8) we can see, that our setup is a bit different from ideal, therefore, we need to correct expression (2.2.6) to obtain real value of the noise current.

From the equivalent circuit of source follower (Figure 3.10) we can see that input voltage, V_{in}, and voltage over gate-source of the first transistor, V_1, are not equal to each other – V_1 is lower because of the negative voltage feedback

$$V_1 = V_{in} - V_{out} = V_{in}(1 - A_V). \quad (3.6)$$

Another factor which changes output current compared to ideal model is that total output current splits in several components between $1/g_m$ and Z_L. It means that current which flows over load, I_L, is lower than total current, I_{total}, produced by nonlinearity in detector

$$I_L = I_{total} \frac{\frac{1}{g_m} \| Z_L}{Z_L}. \quad (3.7)$$

From (2.2.6), (3.6) and (3.7) we can get corrected expression for blocker effect

$$i_{nb}^2 = 2I_{bias}^2 \frac{I_1^2(V_b/V_0)}{I_0^2(V_b/V_0)} \frac{V_{ni}^2}{V_0^2} \left(\frac{\frac{1}{g_m} \| Z_L}{Z_L} \right)^2, \qquad (3.8)$$

where A_V – is given by (3.5).

From (3.8) we can see that increasing of the load impedance, Z_L, decrease level of the output noise current, i_{nb}. To control the influence of the load impedance on the output noise we can connect test resistor, R_{test}, in parallel with amplifier (see Figure 3.11), it will change effective load for a detector. Capacitor C_{test} is used to prevent influence of the resistor R_{test} on operation conditions of the detector.

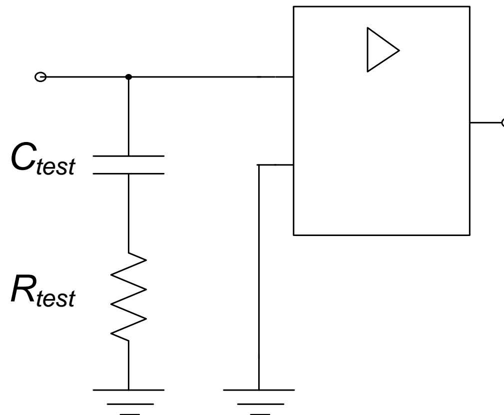

Figure 3.11 Setup for providing measurements with different loads

4. Results

In this chapter we compare theoretical expressions for the envelope detector given in previous chapters with experimental results. Basically there are two blocks of experiments – signal detection and blocker effect. For providing all the experiments we choose 2N7000 transistor, because it has acceptable parameters for building detector. Therefore, this type of transistor has suitable output pins, so it is easy to solder them on mounting board.

4.1 DC measurements

Transistor 2N7000 is an n-channel enhancement mode field-effect transistor. At the Figure 4.1 we see transfer characteristic of saturated transistor in subthreshold region. From this we can find such important parameters of transistor as I_{D0} and V_0 (see expression 2.1.10) – $I_{D0} = 3.6 \cdot 10^{-14}$ A and $V_0 = 77$ mV.

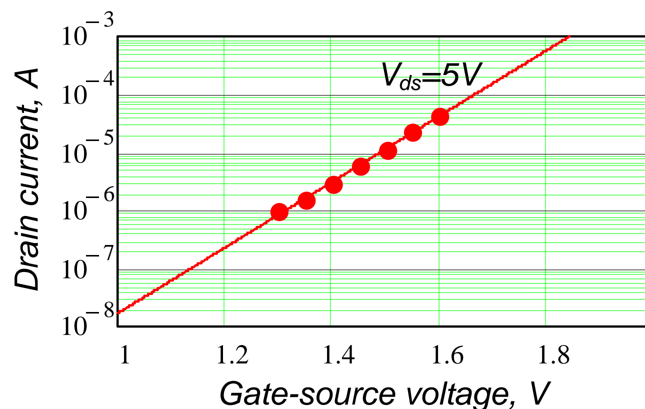

Figure 4.1 Transfer characteristic

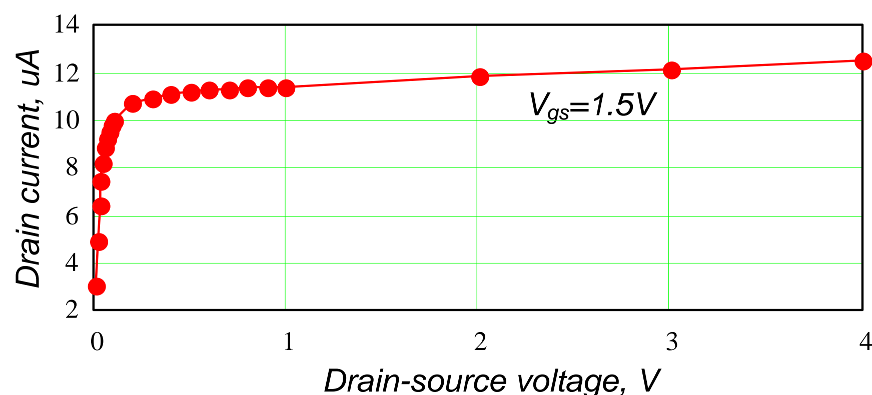

Figure 4.2 Output characteristic

From the output characteristic (Figure 4.2) we can find channel-length modulation parameter, λ (see expression 2.1.9) – $\lambda = 32.26\ \mathrm{V^{-1}}$.

4.2 Signal detection

To provide this measurement we apply AM modulated RF signal, V_{in}, to one of the mixers ports (see Figure 3.1) with carrier frequency f = 10 MHz and modulation frequency f_m

$$V_{in} = V_m \frac{1+\sin\omega_m t}{2}\cos\omega t. \tag{4.1}$$

After that we measure amplitude of the detected signal and plot it together with the output signal predicted by theory, which we can obtain from (2.2.5) using the same correction as in (3.8) (see Figure 4.3)

$$i_{sm} = 4I_{bias}\frac{I_1(V_m/2V_0)I_1(V_m/4V_0)}{I_0(V_m/2V_0)I_0(V_m/4V_0)}\left(\frac{\frac{1}{g_m}\,\|\,R_L}{R_L}\right). \tag{4.2}$$

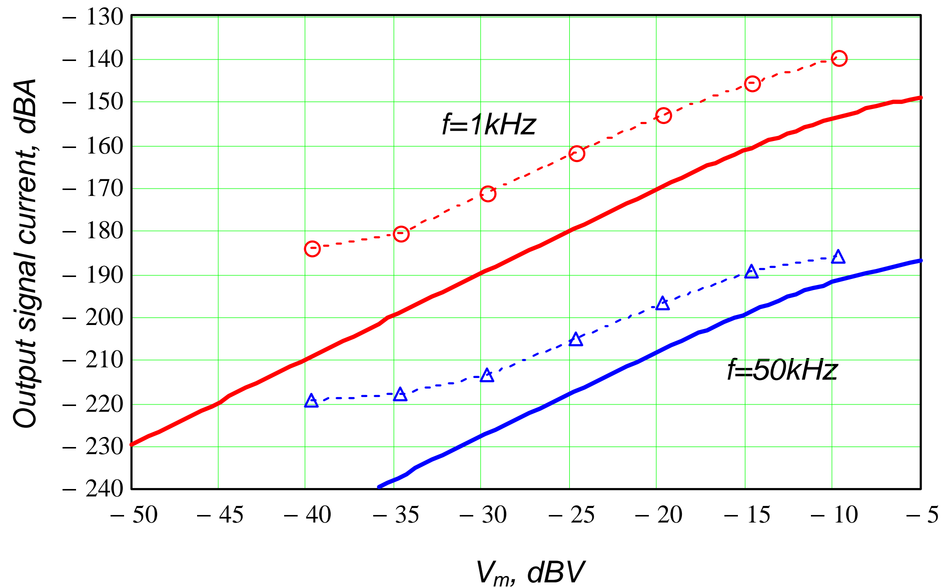

Figure 4.3 Output signal current for envelope detector

From the figure we see that measured values are shifted up compared with theory, but shape of the curves is the same.

4.3 Blocker effect

To provide this measurements we apply blocker signal, V_b, at the frequency 10 MHz and noise, V_{ni}, distributed uniformly in a band ±100 kHz around the blocker.

First experiment is to see blocker effect at different input noise levels. We bias our detector with a current $I_{bias}=10\ uA$ and then sweep blocker signal amplitude at different levels of the input noise, V_{ni}. From the Figure 4.4 we can see that for larger values of input noise even without blocker signal applied part of the noise is being detected, this is self mixing components of the noise.

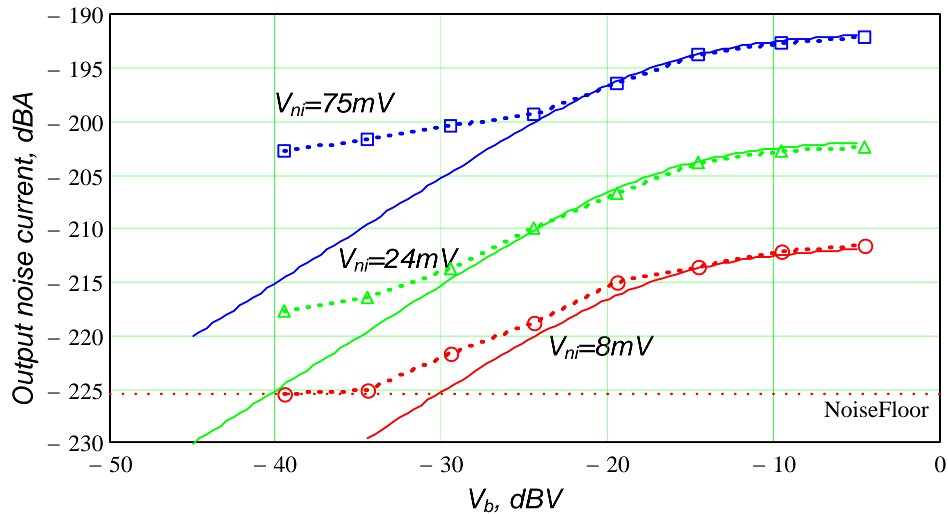

Figure 4.4 Output noise current at different input noise levels

Second experiment is to see blocker effect at different bias conditions of the detector. As we can see from the Figure 4.5 the output current is being compressed compared to changing of bias current, this happens because of negative voltage feedback (see expression 3.8).

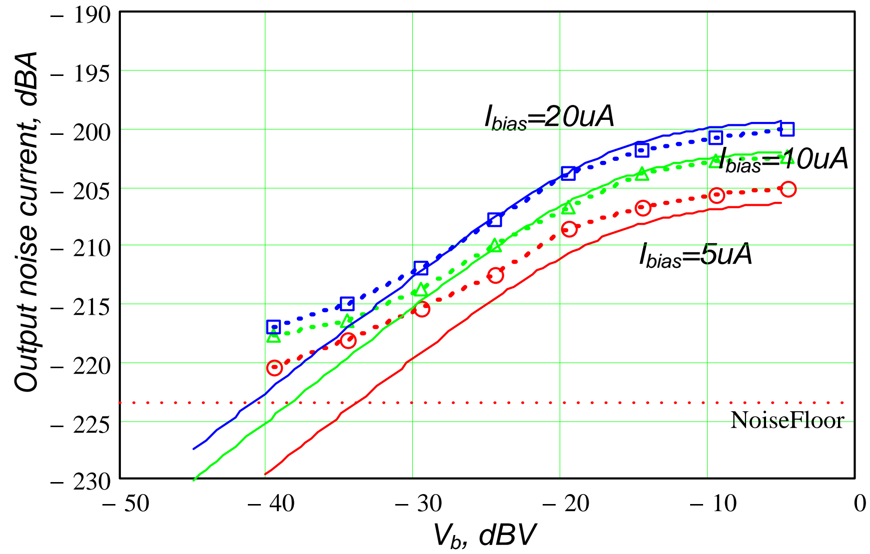

Figure 4.5 Output noise current for different values of bias current

The last experiment is to see influence of the load impedance on the detector output noise current. To provide such measurement we use test resistor (see Figure 3.11), the results are plotted at the Figure 4.6.

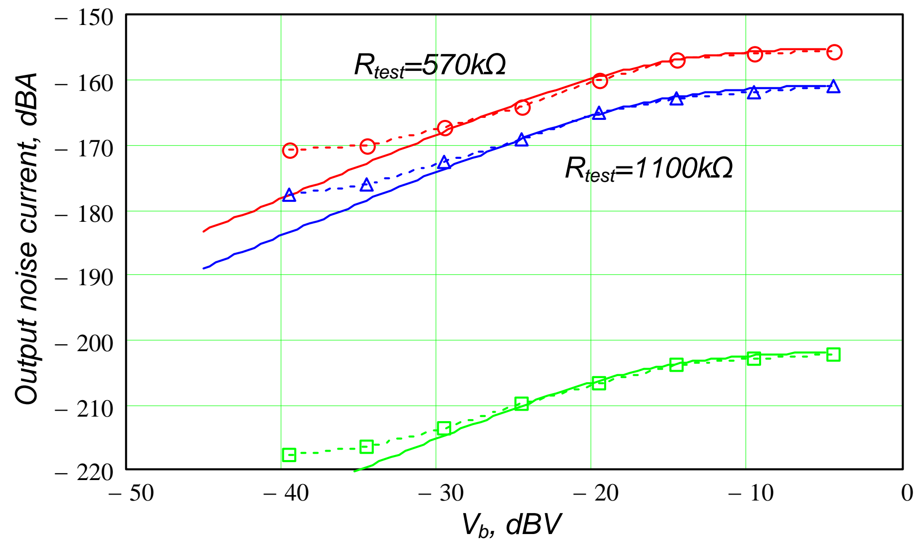

Figure 4.6 Output noise current for different test resistors

5. Conclusion

In this work we have built low power envelope detector and additional blocks for providing measurements. We have also obtained a model of real detector based on two MOS transistors and have compared it with ideal detector.

After providing measurements we compare results with the theory. Results follow well to the change of the circuit parameters and parameters of the input signal. The maximal mismatch between measured and predicted output current is about 10 dB. This could happen due to different reasons – errors in measurements, differences between parameters of the elements in model and in real device or because this model does not perfectly describes our device.

The best sensitivity of the detector that we get is about 1.8 mV for power consumption about 10 uA. These results can be improved by using specific MOS transistors and lumped elements with better parameters at the frequencies of interests.

As for the future work to be done in this subject, firstly, it is necessary to find out the reasons of the difference between theoretical expectations and what we really get during measurements. The main difference between our detector and ideal model is that instead of ideal current source we use another MOS transistor. Probably better understanding of the influence of parasitic transistor parameters and second order effects is needed. The detection process is sophisticated because we have input signal at radio frequency and feedback at low frequency. How does this facts influence the functionality of the detector? Is there anything else in our circuit that can influence the output current in the way we did not expect?

Another way to verify the results is to provide numerical modeling, for example, in Advanced design system [9], and try to find out critical parameters of the circuit which cause this 10 dB difference between theoretical expressions and experimental results.

And, secondly, after solving discussed problems one can build low power envelope detector for specific requirements (particular frequency domain, sensitivity, power consumption) and verify its functionality with measurements.

References

[1] D.C. Daly and A.P. Chandrakasan, “An energy-efficient OOK transceiver for wireless sensor networks”, *IEEE J. Solid-State Circuits*, vol. 42, pp. 1003-1011, May 2007.

[2] R. Meyer, “Low-power monolithic RF peak detector analysis”, *IEEE J. Solid-State circuits*, vol. 30, pp. 65-67, Jan. 1995.

[3] S.M. Sze, *Semiconductor devices: Physics and technology,* SBN/ISSN: 0-471-33372-7, 2 Uppl., Wiley, New York viii, p. 564. , 2002.

[4] A. Prokhorov, O. Gerzheva, “Model of MOSFET in Delphi”, *Halmstad University, Technical report, IDE1066, February 2011*

[5] Emil Nilsson and Christer Svensson, "Envelope Detector Sensitivity and Blocking Characteristics", *European Conference on Circuit Theory and Design (ECCTD 2011), IEEE,* 2011.

[6] B. Razavi, *Design of Analog CMOS Integrated Circuits*. Boston: McGraw-Hill, 2001.

[7] U. Tietze, Ch. Schenk, *Electronic Circuits – Handbook for Design and Applications*, 2nd edition, 2008.

[8] Wikipedia, the free encyclopedia (2011) Laplace transform. [Online]. Available: http://en.wikipedia.org/wiki/Laplace_transform

[9] Agilent (2010) Advanced design system (ADS). [Online]. Available: www.agilent.com/find/ads